

Omni-Directional Mobile Robot Controller Design by Trajectory Linearization

Yong Liu[†], Xiaofei Wu[†], J Jim Zhu[†] and Jae Lew[‡]

[†]School of Electrical Engineering and Computer Science

[‡]Department of Mechanical Engineering

Ohio University

Athens, Ohio 45701

zhuj@ohio.edu

Abstract: In this paper, modeling and nonlinear controller design for an omni-directional mobile robot are presented. Based on the robot dynamics model, a nonlinear controller is designed using the Trajectory Linearization Control (TLC) method. Some simulation results of the controller are presented.

Key Words: mobile robot, nonlinear control, trajectory linearization, omni-direction

1. Introduction

Omni-directional mobile robot is a kind of holonomic robot. Compared with more common car like (nonholonomical) mobile robot, omni-directional mobile robot has the ability to move simultaneously and independently in translation and rotation.[5] The maneuverability of the omni-directional mobile robot makes it widely studied in the dynamic environmental applications. The annual international Robocup competition in which the team of autonomous robots compete in soccer like game, is an example where the omni-directional mobile robot can be used.

The Ohio University (OU) Robocup Team's entry *Robocat* is a cross-disciplinary research project (including ME, EE, CS students and faculties) for Robocup small-size league competition. The current OU Robocup team members are Phase V omni-directional mobile robot, as shown in Figure 1-1. The Phase V *Robocat* is an omni-directional robot with three orthogonal wheels, arranged 120° apart. Each wheel is driven by a DC motors installed with shaft optical encoder. The robot is operated by an PC104 computer with 486 processor running linux operating system. A roof camera over the play field can sense the position and the azimuth angle of robots.

From the robot testing and competition at the Robocup games, it is realized that a precise trajectory control for the robot is one of the key areas to improve the team's performance. The trajectory control of the omni-directional mobile robot can be divided into two tasks, trajectory planning and trajectory following. Trajectory planning is to build a feasible and optimal

geometric path. Trajectory following is to use feedback control to track the path [4]. Since the Robocup robot will work in a dynamic environment, the trajectory following should be able to drive the robot to follow any feasible path.

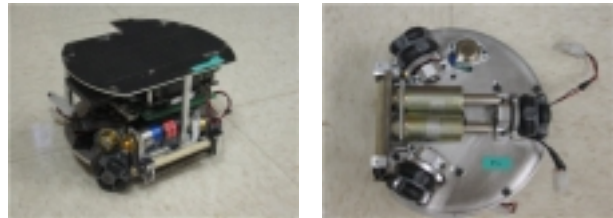


Figure 1-1 Phase V Robocat Robot

It appears that most research on omni-directional mobile robot has been focused on the mechanical design and dynamic analysis. The dynamic model and high precision path following control has not been thoroughly studied. Many omni-directional dynamic models assume that the motor is controlled by an ideal servo, and the motor output torque can perfectly follow the command [7]. However, the motor and servo dynamics constraints can greatly affect the robot behavior, especially when the robot is accelerated and decelerated. In [6] and [11], the dynamic model of the omni-directional mobile robot is developed, and several control strategies for omni-directional mobile robot are discussed. In [6], a resolved-acceleration control with PI and PD feedback is developed. In [11], the PID control, self-tuning PID control, and fuzzy control of omni-directional mobile robot are introduced. The controllers developed in [6] and [11] are based on linear control method while the robot dynamics is nonlinear. Thus, feedback gain of the controllers in [6] [11] have to be tuned to achieve system stability for different trajectory. In [6], gain scheduling is used to assign different feedback gains for different types of trajectory. In [11], adaptive control and fuzzy rules are used to adjust the feedback gain. However, in the dynamic environment such as soccer competition, it is difficult to predetermine the

trajectory and adjust the feedback gain in real time to guarantee both stability and transient response performance of the robot control system. To achieve better performance, a unified trajectory following controller can follow any given feasible trajectories is desired.

In this paper, an omni-directional mobile robot controller using nonlinear control method is developed. The method is based on linearization along a nominal trajectory, and is known as trajectory linearization control (TLC). The TLC combines nonlinear dynamic inversion and linear time-varying eigenstructure assignment in a novel way, and has been successfully applied to missile and reusable launch vehicle flight control systems [8][9][10]. The nonlinear tracking and decoupling control by trajectory linearization can be viewed as the ideal gain-scheduling controller designed at every point on the trajectory. Therefore the TLC provides robust stability and performance along the trajectory without interpolation of controller gains.

In Section 2, the omni-directional mobile robot model is first developed based on the kinematics, dynamics of the robot and the DC motor. Based on this model, in Section 3, a dual-loop controller for the robot is developed using TLC method. In Section 4, simulation tests of the controller are presented, where it is demonstrated that the robot is able to follow three typical trajectories with the same controller gains. Plans for future work are discussed in Section 5.

2 The Omni-Directional Mobile Robot Model

As a first step to develop a robot controller, the equations of robot motion need to be derived. Several simplifying assumptions are made. For example, it is assumed that there is no slip in all the three wheels, and the friction force is simplified to be represented by a viscous friction coefficient. Electrical time constant of the motor is also neglected. It is expected that the feedback controller based on this simplified model can compensate the unmodeled dynamics.

2.1 Coordinates and Symbols

There are two coordinate frames used in the modeling: the body frame (Cartesian frame) and the Earth (World) frame. The body frame is fixed on the moving robot with the origin in the center of chassis, as shown in the figure 2(a). The Earth frame (World frame) is fixed on the play ground, as shown in figure 2(b).

The following symbols are used in the modeling: Wheel 1—rear wheel, Wheel 2—front right wheel, Wheel 3—front left wheel

m – robot mass

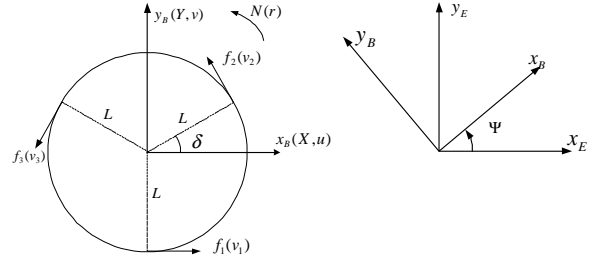
I_z – robot moment inertia

R – wheel radius

L – radius of the body

n – gear ratio

$\omega_{m1}, \omega_{m2}, \omega_{m3}$ – The motor speed



(a) Body frame

(b) Earth (World) frame

Figure 2 Coordinate Frames

Body frame

X, Y – traction forces in the Body frame

N – body rotation torque

r – angular rate of body rotation

u, v – velocity component in the Body frame

$[f_1, f_2, f_3]^T$ – Traction force of the wheels

$[u_1, u_2, u_3]^T$ – Input Voltage of the motors

Earth (World) Frame

x, y – robot location

Ψ – azimuth angle of body

2.2 Robot Dynamics

In the body frame and by Newton's law we have

$$\begin{bmatrix} \dot{u} \\ \dot{v} \\ \dot{r} \end{bmatrix} = \begin{bmatrix} rv \\ -ru \\ 0 \end{bmatrix} + H \begin{bmatrix} X \\ Y \\ N \end{bmatrix}, \quad (2-2-1)$$

where

$$H = \begin{bmatrix} \frac{1}{m} & 0 & 0 \\ 0 & \frac{1}{m} & 0 \\ 0 & 0 & \frac{1}{I_z} \end{bmatrix}, \quad \begin{bmatrix} X \\ Y \\ N \end{bmatrix} = B \begin{bmatrix} f_1 \\ f_2 \\ f_3 \end{bmatrix}$$

and

$$B = \begin{bmatrix} 1 & -\sin(\delta) & -\sin(\delta) \\ 0 & \cos(\delta) & -\cos(\delta) \\ L & L & L \end{bmatrix}.$$

From geometry of mobile robot we have

$$\begin{bmatrix} u \\ v \\ r \end{bmatrix} = (B^T)^{-1} \frac{R}{n} \begin{bmatrix} \omega_{m1} \\ \omega_{m2} \\ \omega_{m3} \end{bmatrix}, \quad (2-2-2)$$

The dynamics of each DC motor can be described using the following equations

$$\begin{bmatrix} \delta u \\ \delta v \\ \delta r \end{bmatrix} = \begin{bmatrix} u_{com} \\ v_{com} \\ r_{com} \end{bmatrix} - \begin{bmatrix} \bar{u} \\ \bar{v} \\ \bar{r} \end{bmatrix} \quad (3-1-4)$$

Linearizing (2-2-5) along the nominal trajectories $[\bar{x}(t), \bar{y}(t), \bar{\Psi}(t)]^T$ and $[\bar{u}(t), \bar{v}(t), \bar{r}(t)]^T$ yields the error dynamics

$$\begin{bmatrix} \dot{e}_x \\ \dot{e}_y \\ \dot{e}_\Psi \end{bmatrix} = A_1 \begin{bmatrix} e_x \\ e_y \\ e_\Psi \end{bmatrix} + B_1 \begin{bmatrix} \delta u \\ \delta v \\ \delta r \end{bmatrix} \quad (3-1-2)$$

where

$$A_1 = \begin{bmatrix} 0 & 0 & -\sin(\bar{\Psi})\bar{u} - \cos(\bar{\Psi})\bar{v} \\ 0 & 0 & \cos(\bar{\Psi})\bar{u} - \sin(\bar{\Psi})\bar{v} \\ 0 & 0 & 0 \end{bmatrix},$$

$$B_1 = \begin{bmatrix} \cos(\bar{\Psi}) & -\sin(\bar{\Psi}) & 0 \\ \sin(\bar{\Psi}) & \cos(\bar{\Psi}) & 0 \\ 0 & 0 & 1 \end{bmatrix}$$

Now stabilizing the tracking error with the proportional-integral (PI) feed back control law

$$\begin{bmatrix} \delta u \\ \delta v \\ \delta r \end{bmatrix} = -K_{p1} \begin{bmatrix} e_x \\ e_y \\ e_\Psi \end{bmatrix} - K_{I1} \begin{bmatrix} \int e_x(t)dt \\ \int e_y(t)dt \\ \int e_\Psi(t)dt \end{bmatrix} \quad (3-1-3)$$

Define the augmented outer loop tracking error vector by

$$\gamma = \begin{bmatrix} \gamma_1 \\ \gamma_2 \\ \gamma_3 \\ \gamma_4 \\ \gamma_5 \\ \gamma_6 \end{bmatrix} = \begin{bmatrix} \int e_x(t)dt \\ \int e_y(t)dt \\ \int e_\Psi(t)dt \\ e_x \\ e_y \\ e_\Psi \end{bmatrix}$$

Then the closed loop tracking error state equation can be written as

$$\dot{\gamma} = A_{1c}\gamma$$

where

$$A_{1c} = \left[\begin{array}{c|c} \mathbf{O}_3 & \mathbf{I}_3 \\ \hline -B_1 K_{I1} & A_1 - B_1 K_{P1} \end{array} \right]$$

where \mathbf{O}_3 denotes the 3×3 zero matrix, and \mathbf{I}_3 denotes the 3×3 identity matrix. Now select K_{I1} and K_{P1} to achieve the desired closed-loop tracking error dynamics

$$A_{1c} = \left[\begin{array}{c|c} \mathbf{O}_3 & \mathbf{I}_3 \\ \hline \text{diag}[-a_{111} & -a_{121} & -a_{131}] & \text{diag}[-a_{112} & -a_{122} & -a_{132}] \end{array} \right]$$

where $a_{1j1} > 0$, $a_{1j2} > 0$, $j = 1, 2, 3$, are the coefficients of the desired closed-loop characteristic polynomial of each channel given by $\lambda^2 + a_{1j2}\lambda + a_{1j1}$. It is easy to verify that

$$K_{I1} = -B_1^{-1} \text{diag}[-a_{111} \quad -a_{121} \quad -a_{131}]$$

$$K_{P1} = B_1^{-1} (A_1 - \text{diag}[-a_{112} \quad -a_{122} \quad -a_{132}])$$

Now the tracking command to the inner loop is given by

$$\begin{bmatrix} u_{com} \\ v_{com} \\ r_{com} \end{bmatrix} = \begin{bmatrix} \bar{u} \\ \bar{v} \\ \bar{r} \end{bmatrix} + \begin{bmatrix} \delta u \\ \delta v \\ \delta r \end{bmatrix}.$$

3.2 Inner Loop Controller

From (2-2-4) the nominal motor control input voltages $[\bar{u}_1(t), \bar{u}_2(t), \bar{u}_3(t)]^T$ for the desired body rate $[\bar{u}(t), \bar{v}(t), \bar{r}(t)]^T$ are given by

$$\begin{bmatrix} \bar{u}_1 \\ \bar{u}_2 \\ \bar{u}_3 \end{bmatrix} = (HB)^{-1} \frac{R \cdot R_a}{k_2 n} G \begin{bmatrix} \bar{u} \\ \bar{v} \\ \bar{r} \end{bmatrix} - (HB)^{-1} \frac{R \cdot R_a}{k_2 n} \begin{bmatrix} rv \\ -ru \\ 0 \end{bmatrix} + B^T \frac{R_a \cdot n}{k_2 R} \left(\frac{k_2 \cdot k_3}{R_a} + b_0 \right) \begin{bmatrix} \bar{u} \\ \bar{v} \\ \bar{r} \end{bmatrix}$$

Defining

$$\begin{bmatrix} e_u \\ e_v \\ e_r \end{bmatrix} = \begin{bmatrix} u \\ v \\ r \end{bmatrix} - \begin{bmatrix} u_{com} \\ v_{com} \\ r_{com} \end{bmatrix}$$

$$\begin{bmatrix} \delta u_1 \\ \delta u_2 \\ \delta u_3 \end{bmatrix} = \begin{bmatrix} u_1 \\ u_2 \\ u_3 \end{bmatrix} - \begin{bmatrix} \bar{u}_1 \\ \bar{u}_2 \\ \bar{u}_3 \end{bmatrix}$$

and linearizing (2-2-4) along the nominal trajectories $[\bar{u}_1(t), \bar{u}_2(t), \bar{u}_3(t)]^T$ and $[\bar{u}(t), \bar{v}(t), \bar{r}(t)]^T$ yield the linearized inner loop tracking error dynamics

$$\begin{bmatrix} \dot{e}_u \\ \dot{e}_v \\ \dot{e}_r \end{bmatrix} = A_2 \begin{bmatrix} e_u \\ e_v \\ e_r \end{bmatrix} + B_2 \begin{bmatrix} \delta u_1 \\ \delta u_2 \\ \delta u_3 \end{bmatrix} \quad (3-1-6)$$

where

$$A_2 = G^{-1} \begin{bmatrix} 0 & \bar{r} & \bar{v} \\ -\bar{r} & 0 & -\bar{u} \\ 0 & 0 & 0 \end{bmatrix} - G^{-1} H B B^T \left(\frac{k_2 \cdot k_3}{R_a} + b_0 \right) \frac{n^2}{R^2}$$

$$B_2 = G^{-1} H B \cdot \frac{k_2 n}{R \cdot R_a}$$

Design the PI feed back control law by

$$\begin{bmatrix} \delta u_1 \\ \delta u_2 \\ \delta u_3 \end{bmatrix} = -K_{p2} \begin{bmatrix} e_u \\ e_v \\ e_r \end{bmatrix} - K_{I2} \begin{bmatrix} \int e_u(t)dt \\ \int e_v(t)dt \\ \int e_r(t)dt \end{bmatrix} \quad (3-1-7)$$

and define the augmented inner loop tracking error vector by

$$\eta = \begin{bmatrix} \eta_1 \\ \eta_2 \\ \eta_3 \\ \eta_4 \\ \eta_5 \\ \eta_6 \end{bmatrix} = \begin{bmatrix} \int e_u(t)dt \\ \int e_v(t)dt \\ \int e_r(t)dt \\ e_u \\ e_v \\ e_r \end{bmatrix}$$

Then the close loop tracking error state equation can be written as

$$\dot{\eta} = A_{2c}\eta$$

where

$$A_{2c} = \left[\begin{array}{c|c} \mathbf{O}_3 & \mathbf{I}_3 \\ \hline -B_2 K_{I2} & A_2 - B_2 K_{P2} \end{array} \right].$$

Now select K_{I2} and K_{P2} to achieve the desired closed-loop tracking error dynamics

$$A_{1c} =$$

$$\left[\begin{array}{c|c} \mathbf{O}_3 & \mathbf{I}_3 \\ \hline \text{diag}[-a_{211} & -a_{221} & -a_{231}] & \text{diag}[-a_{212} & -a_{222} & -a_{232}] \end{array} \right]$$

where $a_{2j1} > 0$, $a_{2j2} > 0$, $j = 1, 2, 3$, are the coefficients of the desired closed-loop characteristic polynomial of each channel given by

$\lambda^2 + a_{2j2}\lambda + a_{2j1}$. It is easy to verify that

$$K_{I2} = -B_2^{-1} \text{diag}[-a_{211} \quad -a_{221} \quad -a_{231}] \quad (3-1-8)$$

$$K_{P2} = B_2^{-1}(A_2 - \text{diag}[-a_{212} \quad -a_{222} \quad -a_{232}])$$

Finally, the control input voltage to the motors are given by

$$\begin{bmatrix} u_1 \\ u_2 \\ u_3 \end{bmatrix} = \begin{bmatrix} \delta u_1 \\ \delta u_2 \\ \delta u_3 \end{bmatrix} + \begin{bmatrix} \bar{u}_1 \\ \bar{u}_2 \\ \bar{u}_3 \end{bmatrix} \quad (3-1-9)$$

4. Simulation

In the simulation, the robot is tested with three different trajectories to follow: (i) a set-point trajectory, (ii) an acceleration trajectory with fixed acceleration rate and (iii) a circular trajectory. These three trajectories are typical trajectories encountered in the real-time competition. The controller can follow these three different trajectories with the same controller gains.

The omni-directional robot can move independently in translation and rotation. The robot has three dimension of freedom (3 DOF). In the simulation, it is shown the controller can effectively decouple and stabilize the robot movement. Unlike many other previous works, which usually use separated translation trajectory and rotation trajectory, in the simulation, the robot can be driven to follow the translation and rotation trajectories simultaneously. Without loss of generality, the initial position of the robot was set to $[0 \ 0 \ 0]$ for all tests, and the robot was stationary in the initial position.

4.1 Location control.

The robot is driven to stop at $[0.05 \ 0.05 \ \pi/4]$ from the origin point. The simulation result is shown in Figure 4-1.

4.2 Acceleration trajectory

In the test, the robot was commanded to accelerate from the original position to the predefined speed $\dot{x} = 0.7 \text{ m/s}$; $\dot{y} = 0.6 \text{ m/s}$; $\dot{\Psi} = 0.1 \text{ rad/s}$ with fixed acceleration rate $\ddot{x} = 0.15 \text{ m/s}^2$; $\ddot{y} = 0.15 \text{ m/s}^2$; $\ddot{\Psi} = 0.02 \text{ rad/s}^2$. The simulation result is shown in figure 4-2.

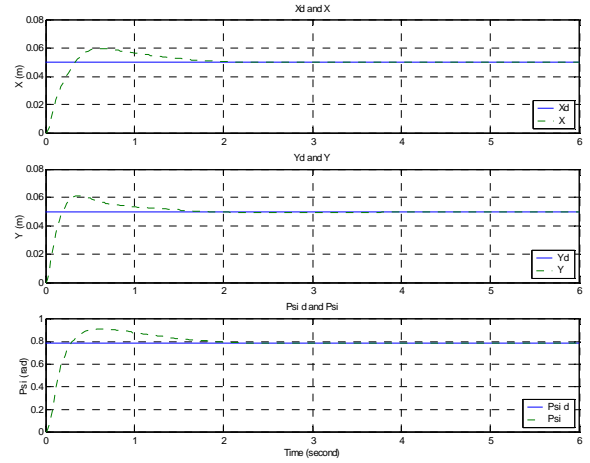


Figure 4-1 Position Control

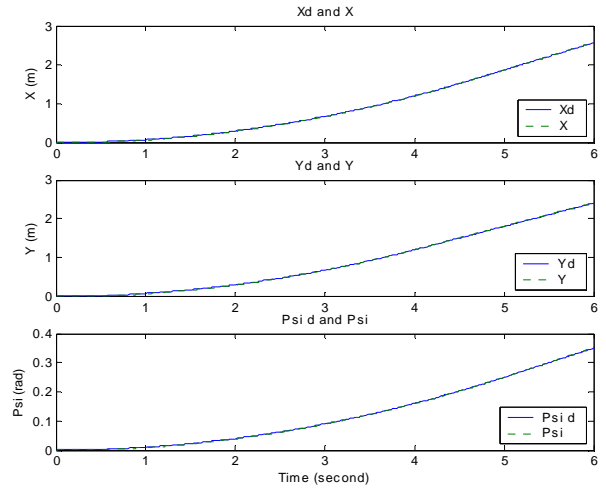


Figure 4-2 Simulation of fixed speed trajectory

4-3 Circular Trajectory

In this test the robot was commanded to accelerate from the initial position and circle around with the angular rate accelerated from 0.05 rad/s to 1 rad/s . The center of the circular trajectory was at $[0 \ -0.5]$, and the robot body was kept facing the tangent direction. The simulation result is shown in Figure 4-3 and

Figure 4-4. Note that in Figure 4-3 the azimuth angle Ψ tracking error is shown on the order of 0.001 radians, and the tracking errors of x and y are on the order of 0.001m.

5. Conclusion and Future Work

In this paper, the equations of motion for an omnidirectional mobile robot are derived based on the robot kinematics, dynamics and the motor dynamics. Based on this model, a novel nonlinear controller using Trajectory Linearization Control (TLC) is designed. The simulation results show that with the same controller gains, the robot can be controlled to follow different trajectories accurately. The robust stability of TLC makes it easy to tune these controller gains.

In this paper only simulation testing results are shown. The next step is to implement and test the controller on the real Robocat robot. Then the controller will be integrated with the vision system and AI system of the Robocat.

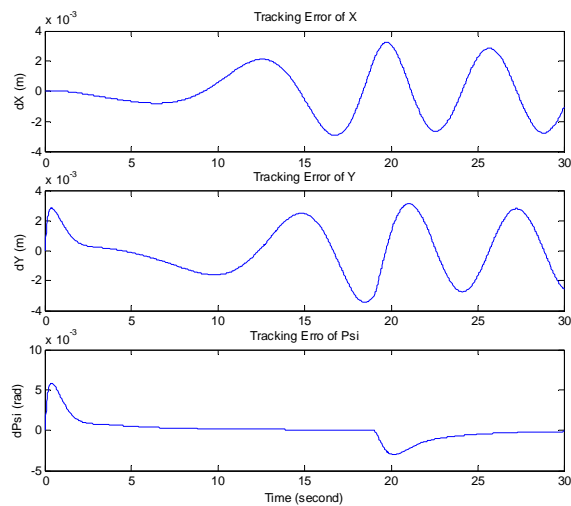


Figure 4-3 Tracking error of Circular Trajectory

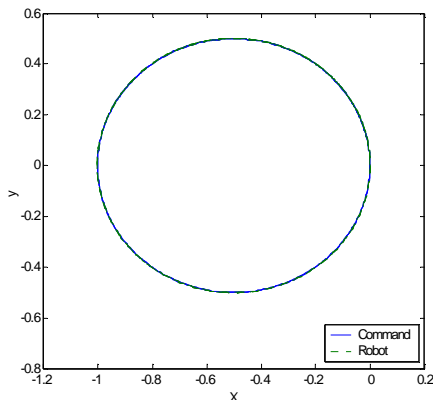


Figure 4-4 Circular trajectory plot of Robot

Acknowledgment. The authors would like to thank Dr. Robert Williams II, Dr. David Chelberg, Dr. Greg Kremer and Dr. Douglas Lawrence for the helpful discussions during this development. Thanks also due to the Ohio University Robocup team member Qiang Zhou, Ted Smith, Matthew Gillen, Mark Tomko, Jianhua Wu and Rui Huang.

References

- [1] L. Wilson , J.Y. Lew and et. "Design and Modeling of a Redundant Omnidirectional RoboCup Goalie," RoboCup 2001 International Symposium, Seattle, WA. August, 2001
- [2] Robert L. Williams II and Brian E. Carter, etc., "Dynamic Model with Slip for Wheeled Omnidirectional Robots," submitted to IEEE TRANSACTIONS ON ROBOTICS AND AUTOMATION, May 2001
- [3] Zhu, J. Jim, "Nonlinear tracking and decoupling by trajectory linearization", a 12-hour lecture with 137 pp. lecture note presented at NASA Marshall space Flight Center, Huntsville, AL. Grant No. NASA/LEQSF (96-01)-01, May 1, 1998-April 30, 1999.
- [4] Tams Kalma-Nagy, Raffaello D'Andrea, Pritam Ganguly, "Near-Optimal Dynamic Trajectory Generation and Control of an Omnidirectional Vehicle."
- [5] Pin, F. G. and Killough, S. M. "A new family of omnidirectional and holonomic wheeled platforms for mobile robots," IEEE Trans. Robotics Automat. 10(2) (1994), 480-C489.
- [6] Watanabe, K., Shiraishi, Y., Tzafestas, S. G., Tang, J. and Fukuda, T., "Feedback Control of an Omnidirectional Autonomous Platform for Mobile Service Robots," Journal of Intelligent and Robotic Systems, 22(3), pp. 315-330, 1998.
- [7] Jong-Suk Choi and Byung Kook Kim, "Near minimum-time direct voltage control algorithms for wheeled mobile robots with current and voltage constraints," Robotica (2001) volume 19, pp. 29-C39.
- [8] J. Zhu, A. Scott Hodel, Kerry Funston and Charles E. Hall, "X-33 entry flight controller design by trajectory linearization - a singular perturbational approach," AAS-01-012, American Astronautical Society Guidance and Control Conference, Breckenridge, Colorado, Jan. 2001, In *Guidance and Control 2001, Advances in the Astronautical Sciences*, Vol. 107, 151-170, American Astronautical Society.
- [9] Zhu, J. Jim, Banker, Brad D. and Hall, Charles E., "X-33 Ascent Flight Controller Design By

- Trajectory Linearization-A Singular Perturbational Approach”, Proceedings, AIAA Guidance, Navigation and Control Conference, Denver, CO, to appear, August, 2000
- [10] Mickle, M.C. and Zhu, J. Jim, “Bank-To-Turn Roll-Yaw-Pitch Autopilot Design Using Dynamic Nonlinear Inversion and PD-eigenvalue assignment”, Proc., 2000 American Control Conference, Chicago, IL, to appear, June 2000
- [11] Keigo Watanabe, Control of Ominidirectional Mobile Robot, 1998 2nd Int. Conf. on Knowledge-Based Intelligent Electronic Systems, 21-23 April 1998, Adelaide, Australia